Age constraints on Lower Paleozoic convection system: Magmatic events in the NW Iberian Gondwana margin

Rubén Díez Fernández [a,*], Pedro Castiñeiras [b], Juan Gómez Barreiro [a]

[a] Departamento de Geología, Universidad de Salamanca, 37008 Salamanca, Spain
[b] Departamento de Petrología y Geoquímica and Instituto de Geología Económica, Universidad Complutense / Consejo Superior de Investigaciones Científicas, 28040 Madrid, Spain

A B S T R A C T

The basal units of the allochthonous complexes of NW Iberia are used to examine the Lower Paleozoic geodynamic evolution of the northern Gondwana margin. These units represent the most external continental margin and the sequence of major magmatic events that affected them has been dated. Isotopic dating and field data highlight the existence of two magmatic pulses, dated at 489 ± 4 Ma (granodiorites) and 474 ± 3 Ma (alkali-granites), and a slightly younger alkaline/peralkaline pulse, dated at ca. 470–475 Ma (alkaline and peralkaline granites). Their framing into the regional background has allowed us to explore the major lithosphere-scale processes developed at the Gondwana periphery at that time, as well as to conceive a consistent model for the opening of the Rheic Ocean that reconciles the timing of sea opening and back-arc extension with the timing of intracontinental rifting. The sequence of events is framed in a Cambrian and Ordovician peri-Gondwanan subduction setting where we also explore how subduction may be linked to coeval intraplate magmatism far inboard of the arc–trench. This contribution discusses how such a scenario can be traced in basement areas through a modern analog perspective.

Keywords:
Convection
Mantle dynamics
Plume
Gondwana
NW Iberia

1. Introduction

The analysis of the sedimentary basins and magmatic provinces preserved as deformed allochthonous and autochthonous sequences in the Variscan belt traces the Lower Paleozoic geodynamic evolution of the European Gondwana lithosphere. In Iberia, both the sedimentary and the igneous rocks register the Cadomian cycle (Eguiluz et al., 2000; Rodríguez-Alonso et al., 2004), followed by the opening of the Rheic Ocean (Sánchez Martínez et al., 2009), and its subsequent closure during the Upper Paleozoic (Martínez Catalán et al., 2007).

There is wide evidence from the igneous record that continental rifting affected the Iberian margin during the Lower Paleozoic (Ribeiro and Floor, 1987; Pin et al., 1992; Rodríguez Aller, 2005). Interestingly, its timing (ca. 470–480 Ma; Rodríguez et al., 2007) is about 10–20 m.y. younger than the estimated age for the opening of the Rheic Ocean (ca. 490–500 Ma; Pin and Carme, 1987; Ménot et al., 1988; Franke, 1995; Kemnitz et al., 2002; Nance et al., 2002; Timmermann et al., 2006; Arenas et al., 2007; Linnemann et al., 2007; Kryza and Pin, 2010; Pedro et al., 2010). Notwithstanding, it is widely accepted that this rifting event is related to a large gravitational pull on the Gondwana margin provided by subduction of the Iapetus-Tornquist lithosphere. This setting produced new oceanic lithosphere at the Gondwana periphery by sea-floor spreading in back-arc systems, and promoted the drifting of peri-Gondwanan terranes, thus giving birth to the Rheic Ocean in their wake (Nance et al., 2010).

Any model advanced to explain this sequence of events must also consider the fact that a similar evolution has been reported in the Variscan belt in France (Crowley et al., 2000; Ballèvre et al., 2009 and references therein), central Europe (Narebski et al., 1986; Furnes et al., 1989; Dörr et al., 1998; Floyd et al., 2000; Franke, 2000; Linnemann et al., 2007), Corsica, and Sardinia (Ricci and Sabatini, 1978). These regional data record an evolution in time across (not just along) the continental margin. In continental-arc settings, the transference of slab-pull forces from the arc–trench to the continent is limited once their connection throughout the arc edifice is lost. In the European sections of Gondwana, either ridge incision or the establishment of a back-arc spreading centre is younger than the continental rifting. Indeed, the extension of the continental margin continued afterwards (Prigmore et al., 1997; Stampfli et al., 2002). For this reason, although rollback is considered the major mechanism promoting the drifting of the European peri-Gondwanan terranes, there is no model that explains the source of tensional forces on the continental lithosphere after they pulled apart. The aim of this article is to explore the origin of such forces by trying to couple the rifting record with mantle dynamics in an ancient subduction setting.

The basal units of the allochthonous complexes of NW Iberia represent a coherent continental block accounting for the Lower

* Corresponding author. Tel.: +34 923 294488; fax: +34 923 294514.
E-mail addresses: georuben@usal.es (R. Díez Fernández), castigar@geo.ucm.es (P. Castiñeiras), jugb@usal.es (J. Gómez Barreiro).

Paleozoic evolution of a piece of the Gondwana margin. We present U–Pb SHRIMP age constrains on the major tectonomagmatic events that affected this section in order to explore the links between volcanic-arc systems, ocean opening, and intraplate igneous activity through a lithosphere-scale perspective. The results are discussed and integrated on the basis of field observations, regional background and modern analogues.

2. The northern Gondwana margin in NW Iberia

The Late Neoproterozoic to Carboniferous geodynamic evolution of the European Gondwana margin is preserved in the Variscan belt (Fig. 1a). The broad restoration of its major tectonostratigraphic domains allows the paleogeographic distribution of crustal provinces to be set (e.g. Von Raumer et al., 2002; Stampfli et al., 2011). The inner

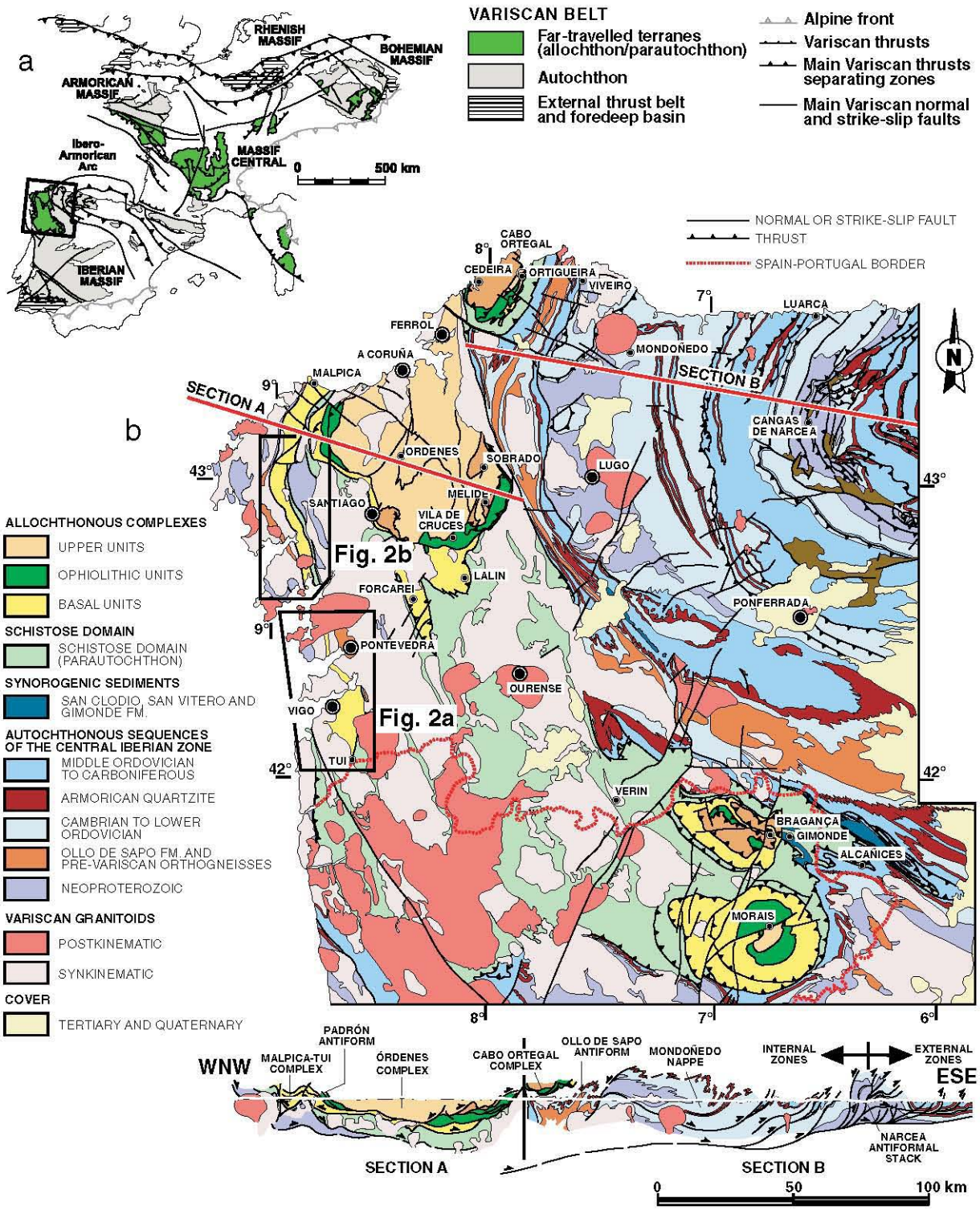

Fig. 1. (a) Synthesis of the major domains of the Variscan belt and location of the study area. (b) Map and composite cross-section showing the allochthonous complexes and the parautochthonous and autochthonous sequences in NW Spain.

parts of Gondwana are represented by the autochthonous sequences of the Iberian Massif (Fig. 1a). Some of the boundaries of the major domains acted as transform-like faults during the Variscan collision (Martínez Catalán, 2011). To reduce the uncertainties related to lateral tectonic movements, we will focus on NW Iberia and, in particular, on the easily restorable thrust stack defined, from bottom to top, by the Central Iberian Zone, the Schistose Domain and the lower sections of the allochthonous complexes (Fig. 1b; Martínez Catalán et al., 2007).

2.1. Sediments and magmatism

In the autochthonous sequences of the Central Iberian Zone (Fig. 1b), the establishment of a Lower Paleozoic passive continental margin followed Neoproterozoic Andean-type activity (Cadomian cycle) (Rodríguez-Alonso et al., 2004). Extensional activity produced high subsidence rates from the Middle Cambrian to Late Ordovician (von Raumer and Stampfli, 2008). Although local Early Ordovician unconformities may exist (e.g. Díez Balda et al., 1990), the sedimentation was generally continuous during this time interval (e.g. Díez Montes et al., 2010). Volcanism occurred from the Cambrian to the Silurian, with a maximum in the Early Ordovician (470–480 Ma), when the younger constituents of the volcanic and volcaniclastic Ollo de Sapo Formation erupted (Montero et al., 2009b; Díez Montes et al., 2010). Coeval widespread intrusive magmatism affected the Lower Cambrian and Neoproterozoic successions (e.g. Solá et al., 2005; Bea et al., 2006; Castiñeiras et al., 2008; Talavera et al., 2008; Liesa et al., 2011).

The Schistose Domain (Fig. 1b) represents a more external section of the continental margin (Martínez Catalán et al., 1999). This domain occupied an intermediate position between the autochthonous sequences of the Central Iberian Zone and the allochthonous complexes. Also referred to as the Parautochthon, the Schistose Domain is a Variscan imbricate thrust sheet composed of rare volcanic rocks and a siliciclastic sedimentary sequence (Marquínez García, 1984; Barrera et al., 1989; Ribeiro et al., 1990) that shows good stratigraphic correlation with the autochthonous sequences of the Central Iberian Zone (Farias et al., 1987). Felsic to mafic metavolcanics occur in the Schistose Domain (e.g. Ferragne, 1972; Arenas, 1988; Meireles, 2000). Even though this magmatism is uncommon, it shows a geochemical evolution from calc-alkaline and high-K (shoshonitic) magmatism to alkaline anorogenic rhyolites, the latter suggesting crustal extension during the Arenig (475 ± 2 Ma; Arenas, 1984; Gallastegui et al., 1987; Ancochea et al., 1988; Valverde-Vaquero et al., 2005).

The most external Paleozoic continental margin rests over the autochthonous sequences and the Schistose Domain. It is represented by the basal units of the allochthonous complexes (Fig. 1b). These units are composed of Late Neoproterozoic and Lower to Middle Cambrian sedimentary rocks. The Neoproterozoic succession was intruded by Lower Cambrian granitoids as well as by anorogenic Ordovician magmatism. The Neoproterozoic succession was deposited during the last pulses of the Cadomian cycle, whereas the overlying Lower–Middle Cambrian succession was not intruded by granitoids, and records, together with the lowermost ophiolitic units of NW Iberia, the development of a back-arc basin at the edge of Gondwana (Arenas et al., 2007; Díez Fernández et al., 2010). This basin developed during the pulling apart of a continental volcanic arc (Abati et al., 1999; Andonaegui et al., 2002; Fuenlabrada et al., 2010), which was emplaced on top of the allochthonous pile of NW Iberia (e.g. Gómez Barreiro et al., 2007) and Europe (e.g. Ballèvre et al., 2009) during the Variscan cycle.

2.2. Selected area and geochronological background

Among the sections of the margin described above, the basal units of the allochthonous complexes are particularly suited to the analysis of rift–drift processes and magmatic events developed in the Gondwana periphery. This is because they were widely affected by rift-related magmatism during the Lower Paleozoic, and the building of the continental volcanic arc may have left a fingerprint here as well. In addition, the regional background allows for easy correlation of these events with the record of the inner sections of the continent.

The igneous assemblages of the basal units have been the focus of isotope geochronological work since the 1960s (Floor, 1966; Van Calsteren et al., 1979; García Garzón et al., 1981; Pin et al., 1992; Santos Zalduegui et al., 1995; Montero et al., 1998; Rodríguez et al., 2007; Montero et al., 2009a; Abati et al., 2010). The time interval over which the entire period of magmatism affecting this continental section took place (470–500 Ma) has not changed since the earliest studies, although progressive refinement has been achieved. There is a calc-alkaline association (see Rodríguez Aller, 2005) ranging in age from about 490 to 500 Ma (Abati et al., 2010), and an alkaline association with an age range of 470–485 Ma (Rodríguez et al., 2007; Montero et al., 2009a). However, it is still not clear whether or not there is a direct link between age and geochemical affinity. Indeed, the calc-alkaline association may span the entire 470–500 Ma time interval.

Arps (1970), Floor (1966) and Rodríguez Aller (2005) highlighted the existence of several igneous rock types, which were grouped in two associations: a calc-alkaline group including tonalites, granodiorites and alkali-granites (high-K), and an alkaline association with alkaline and peralkaline granites and quartz syenites. The granodiorites show gradual transitions to dioritic and trondhjemitic rocks, and may include igneous enclaves of monzonite, trondhjemite and diorite. The rocks of the calc-alkaline association may have lenses of mafic rocks (alkaline to sub-alkaline basalts and gabbros), whereas the alkaline association may contain syenites and fine-grained mafic enclaves (Pin et al., 1992; Rodríguez Aller, 2005).

All of the rock types, including the sedimentary and the igneous rocks, are exposed together in the Malpica-Tui Complex, which was selected for field analysis and rock sampling (Fig. 2).

2.3. Relative geochronology

The Variscan overprint is strong but heterogeneous and transformed the pre-Variscan igneous rocks into variably deformed orthogneisses. In this section, we will refer to all of these rocks using the nomenclature of their undeformed protoliths. Field observations provide constrains on the relative chronology of some of the igneous protoliths. The lack of lenses of metabasites within the alkaline and peralkaline granites strongly suggests that these two rock types are the youngest constituents of the Lower Paleozoic igneous assemblage. Such lenses do occur in the rest of the igneous and sedimentary rocks, and chilled margins and local exposures indicate they represent dyke swarms.

No field criteria establishing the mutual relationships between the alkaline and peralkaline granites have been found, but gradual transitions suggest they were mostly coeval. The restoration of the Variscan deformation in the southern section of the Malpica-Tui Complex suggests that the peralkaline granites represent ring dikes (Díez Fernández and Martínez Catalán, 2009). Furthermore, both the alkaline and peralkaline granites run either along the borders of other igneous massifs, or show strong obliquity relative to them (Fig. 2), suggesting that their distribution was mainly controlled by faults or other pre-intrusion anisotropy, and that they post-date the calc-alkaline association.

The alkaline granites include mesocratic (Sample MTG-10) to melanocratic facies, which are much less abundant. The melanocratic facies (syenites and alkali-feldspar syenites) may occur as xenoliths in the mesocratic granites. Floor (1966) identified three facies of peralkaline granites. Two of these are meso- to melanocratic marginal facies (Zorro and Magnetite facies), and show minor chemical differences (Montero et al., 1998) and gradual transitions to the most common, leucocratic facies (Galiñeiro facies, Sample MTG-6).

The relationships between the tonalites (A Pioza tonalitic orthogneiss), granodiorites (MTG-7) and alkali-granites (MTG-3 and MTG-4)

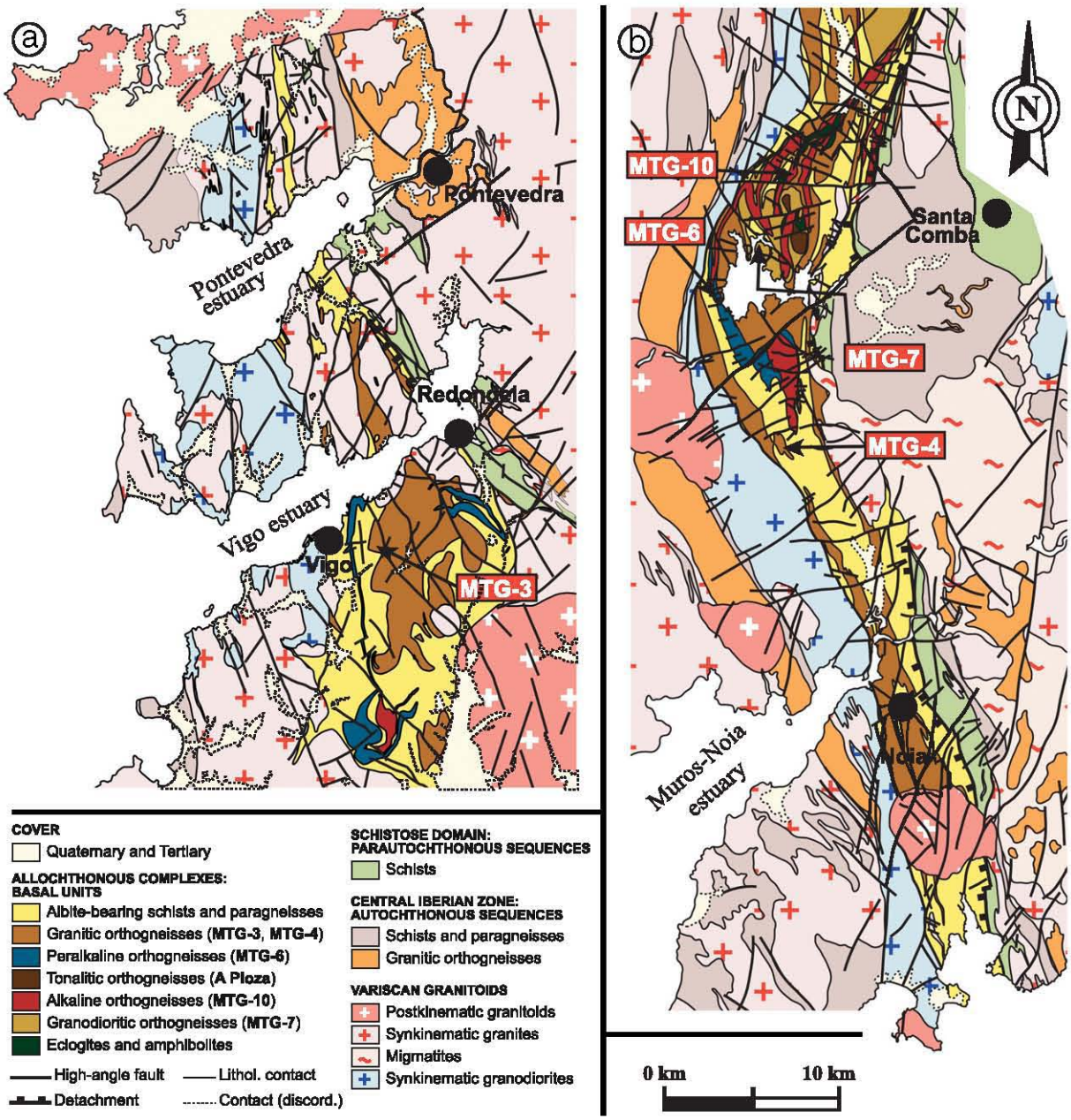

Fig. 2. (a) Southern and (b) Central sections of the Malpica-Tui Complex in Galicia, NW Spain. See regional position in Fig. 1b. The sample location is included.

of the calc-alkaline association cannot be clearly established in the field. Mapping of the alkali-granite massifs reveals the existence of small patches of granodiorites in both the core and close to the rims of the massifs. However, exposures good enough to confirm the xenolithic character of these patches have not been found. Rodríguez Aller (2005) reported enclaves of tonalite and tonalite–diorite within the granodioritic massifs. These data may be used to asses a preliminary relative chronology in the calc-alkaline association, the tonalites and alkali-granites being the oldest and the youngest constituents, respectively.

3. U–Pb SHRIMP analysis

3.1. Structural framework and rock sample description

The external margin of Gondwana was affected by five main phases of deformation during the Variscan cycle (Díez Fernández et al., 2011). It was subducted beneath an accretionary prism and Laurussia (D_1), and subsequently exhumed and emplaced onto the adjacent mainland of Gondwana (D_2). The subduction-exhumation process transformed the pre-Variscan record into a layered tectonostratigraphy consisting of foliated metasedimentary rocks and metabasites alternating with large, lens-shaped, massifs of orthogneisses and metaigneous rocks, which are the focus of this study. Early exhumation was followed by the development of an out-of-sequence thrust system (D_3; Martínez Catalán et al., 2002). Crustal thickening triggered the extensional collapse of the orogenic belt (D_4; Martínez Catalán et al., 2002; Gómez Barreiro et al., 2010; Díez Fernández et al., accepted for publication), which was later affected by strike-slip tectonics (D_5; Martínez Catalán et al., 2009).

Five samples from the igneous assemblage of the basal units, namely MTG-3, 4, 6, 7 and 10, were selected for U–Pb SHRIMP analysis on zircon (see sample locations in Supplementary Tables and KML

file). All but MTG-10 show a gneissic foliation and a mineral lineation formed by an alternation and alignment of quartzo-feldspathic bands and ferromagnesian minerals, depending on the composition. D_1 metamorphism reached eclogite facies conditions in the sampling areas, while the subsequent exhumation developed under medium temperature amphibolite facies to low pressure greenschist facies conditions (Díez Fernández et al., 2011 and references therein).

Sample MTG-7 is a granodiorite orthogneiss consisting of stretched plagioclase pseudomorphs (zoisite/clinozoisite, phengite, jadeite, and granoblastic plagioclase), quartz, biotite, and minor quantities of K-feldspar, allanite, opaque minerals, white mica, chlorite (low temperature retrogression), zircon, tourmaline, and monazite. Biotite is usually surrounded by D_1 coronitic garnet.

Samples MTG-3 and MTG-4 are alkali-granite augen orthogneisses. Their mineralogy comprises augen K-feldspar, quartz, plagioclase and biotite, and minor quantities of green amphibole, epidote, garnet, white mica, titanite, chlorite, rutile, opaque minerals, allanite, zircon, and apatite.

Sample MTG-10 is a weakly deformed alkaline metagranite consisting of albite, quartz, K-feldspar, and variable amounts of green amphibole (hastingsite), biotite, epidote, titanite, garnet, white mica, zircon, apatite, allanite, fluorite, magnetite and opaque minerals. Sample MTG-6 is a peralkaline granite orthogneiss. The quartzo-feldspathic fraction is similar to that of the alkaline granites, but the main melanocratic constituents are riebeckite, aegirine, astrophyllite and annitic biotite. Other minor constituents are zircon, titanite, sulphides, fluorite, magnetite, ilmenite and REE- and HFSE-saturated phases (Montero et al., 1998).

Samples MTG-3, 6, and 7 show a flat-lying S_2 gneissic banding and D_2 stretching and crenulation lineation, whereas the main tectonic fabric in sample MTG-4 is a subvertical low-grade crenulation cleavage (S_5) accompanied by a D_5 subhorizontal stretching and crenulation lineation. Petrographic analysis in weakly deformed protoliths and tectonites suggests that these pre-Variscan granitoids had phaneritic-holocrystalline texture. The texture was hypidiomorphic inequigranular in the granodiorites, porphyritic inequigranular in the alkali-granites (K-feldspar phenocrysts), and medium to fine-grained inequigranular in the alkaline and peralkaline granites, all of which suggest shallow emplacement levels (Rodríguez Aller, 2005).

An additional sample was collected in the A Pioza tonalitic orthogneiss (494 ± 3 Ma, U–Pb in zircon; Abati et al., 2010). The complexity of the results far exceeds the objective of this article and will be treated in more detail separately (Castiñeiras et al., in prep.).

3.2. Analytical techniques

Zircon separation was carried out at the Universidad Complutense (Madrid) following standard techniques, including crushing, pulverizing, sieving, Wilfley table, magnetic separator and methylene iodide.

Zircon was handpicked under a binocular microscope at the Stanford-US Geological Survey micro analytical center (SUMAC). In the granodiorite and alkali-granite samples, the stubbier grains were selected to seek inheritance; in the alkaline and peralkaline gneisses the zircon grains selected were the most transparent. Zircon was mounted on glass slides with a double-sided adhesive in 1×6 mm parallel rows together with some grains of zircon standard R33 (Black et al., 2004) and set in epoxy resin. After the resin was cured, the mounts were ground down to expose their central portions by using 1500 grit wet sandpaper and polished with 6 μm and 1 μm diamond abrasive on a lap wheel. Prior to isotopic analysis, the internal structure, inclusions, fractures and physical defects were identified with transmitted and reflected light on a petrographic microscope, and with cathodoluminescence (CL; Fig. 3) on a JEOL 5600LV scanning electron microscope. In sample MTG-6, the images were taken in backscattered electrons owing to the absence of luminescence in their zircon grains. Following the analysis, secondary electron images were taken to determine the exact location of the spots.

U–Th–Pb analyses of zircon were conducted on the Bay SHRIMP-RG (Sensitive High Resolution Ion Microprobe-Reverse Geometry) operated by the SUMAC facility (USGS-Stanford University) during several analytical sessions from May through September 2008.

U–Th–Pb analytical procedures for zircon dating follow the methods described in Williams (1997). Secondary ions were generated from the target spot with an O_2- primary ion beam varying from 4–6 nA. The primary ion beam produced a spot with a diameter of ~25 μm and a depth of 1–2 microns for an analysis time of 12–13 min. Data for each spot were collected utilizing five or four cycle runs through the mass stations, depending on the presumed origin (magmatic or inherited, respectively) of the selected target. In the magmatic zones, the counting time for ^{206}Pb was increased according to the Paleozoic age of the samples to improve counting statistics and precision of the $^{206}Pb/^{238}U$ age. The isotopic compositions were calibrated against R33 ($^{206}Pb^*/^{238}U = 0.06716$, equivalent to an age of 419 Ma, Black et al., 2004) which was analyzed every fourth analysis.

Data reduction was carried out using Squid software (Ludwig, 2002), which follows the methods described by Williams (1997), and Ireland and Williams (2003), and Isoplot software (Ludwig, 2003) was used to create the graphs. Ages older than 1000 Ma are reported based on $^{207}Pb/^{206}Pb$ ratios, corrected for common Pb using the ^{204}Pb method, whereas younger ages are reported using the $^{206}Pb/^{238}U$ ratios corrected for common Pb with the ^{207}Pb method. The Pb composition used for initial Pb corrections ($^{204}Pb/^{206}Pb = 0.0554$, $^{207}Pb/^{206}Pb = 0.864$ and $^{208}Pb/^{206}Pb = 2.097$) was estimated from Stacey and Kramers (1975). Analytical results are presented in Supplementary Tables 1–5 (available from journal website) and plotted in Tera-Wasserburg and probability density diagrams.

4. Zircon description

Zircon in sample MTG-7 (granodiorite orthogneiss) forms small colorless grains with varied habits from simple dipyramidal prisms to multifaceted grains, all with lustrous surfaces. In sample MTG-3 (alkali-feldspar granite orthogneiss), zircon is colorless or faintly colored, with both lustrous and dull surfaces. Most of the grains are elongated prisms with high length-to-width ratios (2–3:1), and are usually broken. Cathodoluminescence images of zircon from samples MTG-7 and 3 display internal areas with an assortment of textures typical of inherited cores surrounded by poorly luminescent rims (Fig. 3). The xenocrystic cores may be made up of several concentric zones with variable luminescence. Zoning in these areas is usually oscillatory, but homogeneous, sector and soccer ball zoning can also be found. The shape of the cores is mainly rounded, with subordinate irregular or angular shapes. The rims are generally less luminescent than the cores and have oscillatory and homogeneous zoning. The zoning pattern of the rims usually truncates the core zoning, although some grains show a continuous growth between core and rim.

In sample MTG-4 (alkali-feldspar granite orthogneiss), zircon is light brown in color with rough surfaces. They form dipyramidal prisms with simple habits and length-to-width ratios of 2:1. The size of the crystals is usually around 0.1 mm, although a larger population also occurs (~1 mm). CL images from this sample reveal poorly luminescent zircons with faint oscillatory zoning (Fig. 3). The most striking characteristic of these zircon grains is the absence of obvious xenocrystic cores, even though the stubbier grains were selected to maximize their presence.

The zircon yield in the alkaline and peralkaline gneisses is considerably greater than that of the granodiorite and alkali-granite gneisses. In sample MTG-10 (alkaline gneiss), zircon forms large brownish dipyramidal prisms, usually broken. Under CL, zircon is moderately luminescent and shows well-developed oscillatory zoning, although homogeneous central areas can also be found (Fig. 3). In sample MTG-6 (peralkaline gneiss), zircon occurs as large reddish

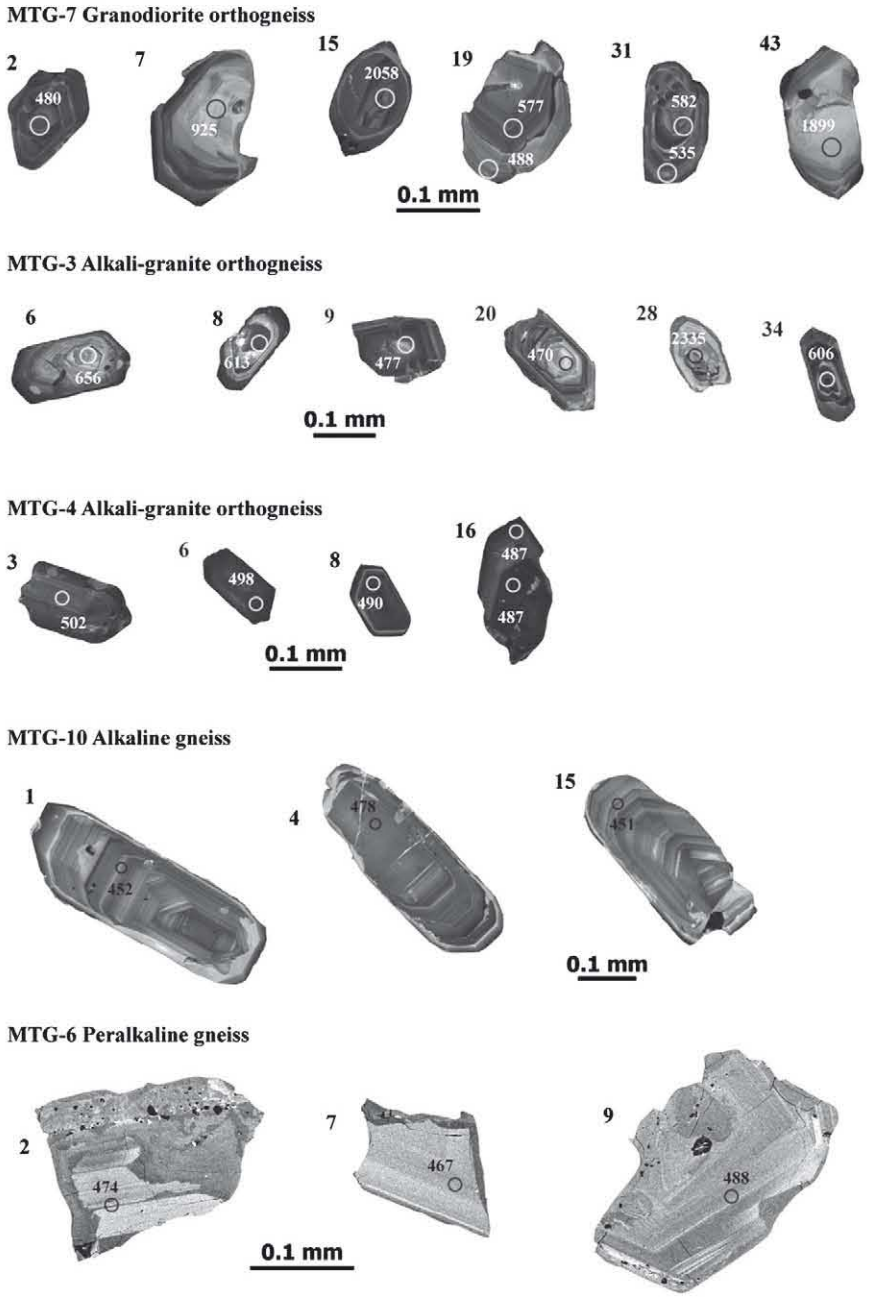

Fig. 3. (CL) Cathodoluminescence images for selected zircons from the studied samples, with the location of the SHRIMP spots and the age in Ma.

broken fragments, in which some pyramids can be distinguished but prisms are lacking or not readily recognizable. Zircons grains are translucent due to the amount of inclusions and have rough surfaces. CL images reveal that zircon in sample MTG-6 is non-luminescent and backscattered images were taken to reveal the internal structure. Most of the zircon fragments have homogeneous zoning, but oscillatory zoning can be recognized in some grains (Fig. 3). Backscattered images also exhibit areas full of small inclusions.

5. U–Pb results

5.1. Granodiorite orthogneiss

Fifty-seven analyses were obtained from 48 zircon grains from sample MTG-7 (Supplementary Table 1). Eight analyses were rejected due to either high common ^{206}Pb (>1.5%), cracks or discordance higher than 10%. The remaining 49 analyses are plotted in two density probability diagrams (Fig. 4a and b). Twenty-eight analyses of xenocryst cores yield ages spanning from 3075 to 512 Ma. Twelve additional analyses fall in class intervals older than ~505 Ma, but they were obtained from non-xenocrystic inner zones or even discordant rims. These data are also considered inheritance, even though the zircon zones do not correspond to obvious inherited cores. From the total of 40 inherited ages, the most important populations are 2050 Ma (four analyses), 2010 Ma (four analyses), 580 Ma (five analyses) and 565 Ma (seven analyses). Other old age components are only represented by one to three analyses (Fig. 4a).

The youngest set of analyses in this sample clusters around a concordia age of 489 ± 4 Ma (Fig. 4b and c) with a mean square of weighted deviation for concordance (MSWD) equal to 1.15. This result is

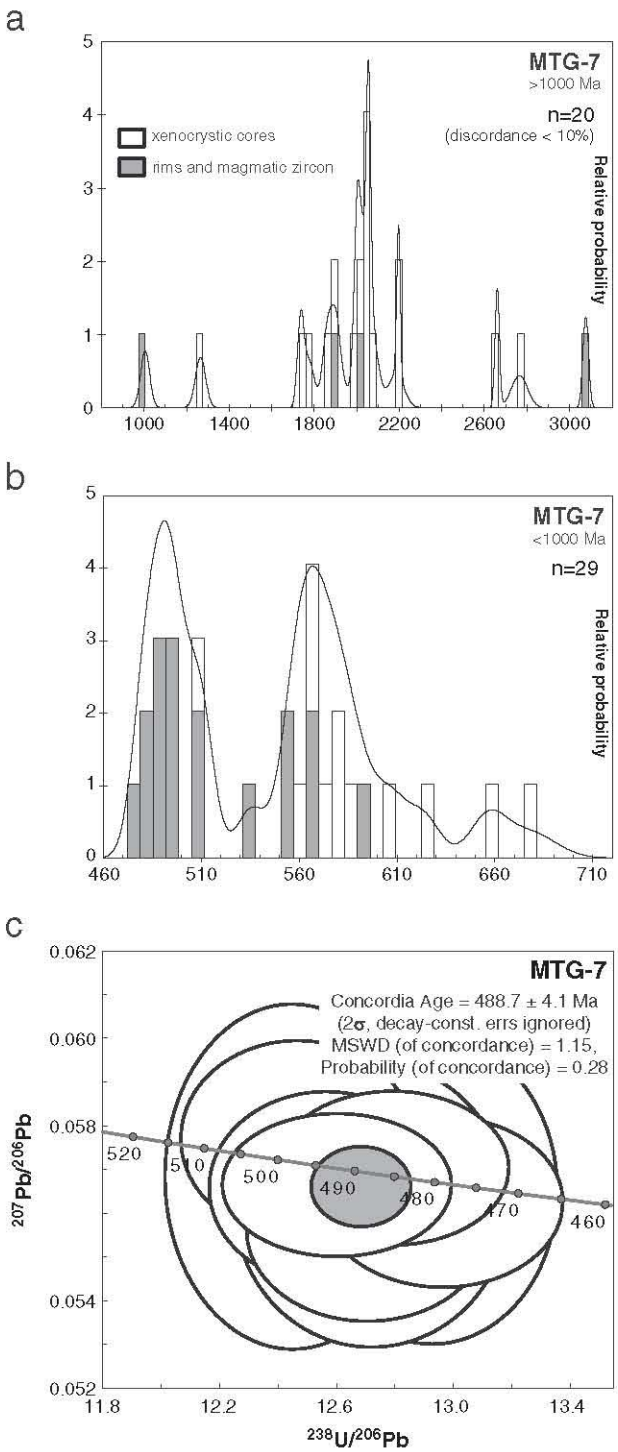

Fig. 4. Relative probability density plots for sample MTG-7. (a) Age data older than 1.0 Ga is given as ^{204}Pb-corrected ^{207}Pb/^{206}Pb, whereas (b) young data is given as ^{207}Pb-corrected ^{206}Pb/^{238}U. (c) Tera-Wasserburg plot showing SHRIMP U–Pb ages from the most concordant zircons in sample MTG-7. The light grey ellipse represents the concordia age calculated by Isoplot.

considered the best estimate for the crystallization age of the granodiorite protolith.

5.2. Alkali-granite orthogneisses

In sample MTG-3, only 4 analyses were obtained from inherited cores with ages higher than 1000 Ma. Two of them have discordance >10%, whereas the other two yield ages of 1.9 and 2.2 Ga. Thirty analyses yield ages lower than 1000 Ma, nine of them have high common Pb (between 0.8 and 9%, see Supplementary Table 2) and are not considered further. The remaining 21 analyses span the interval 655–460 Ma (Fig. 5a). In this sample, only the oldest four ages (from 656 to 593 Ma) were obtained from xenocrystic cores. The rest of the analyses are distributed in three major populations (Fig. 5b) at 530 Ma (3 analyses), 505 Ma (five analyses) and 475 Ma (9 analyses). The best estimate for the crystallization age of the igneous protolith of this sample is a concordia age of 474 ± 3 Ma (MSWD = 0.15, Fig. 5c). This age is obtained by considering only the most concordant analyses with the lowest common Pb content (<0.3%).

In sample MTG-4, the most luminescent areas were selected for analysis to avoid U-rich, non-luminescent zircon. Seventeen analyses were obtained from 16 zircon grains. Even though we aimed at inner areas of the zircon grains to obtain inheritance data, ages span only from 470 to 505 Ma (Supplementary Table 3). The youngest analysis is equivalent to the magmatic age of sample MTG-3 (~475 Ma), whereas four older analyses (~505 Ma) could represent the inherited component found in the same sample. However, most of the analyses pool together to obtain a mean age of 490 ± 3 Ma (MSWD = 1.5, Fig. 6), equivalent to the age obtained in sample MTG-7.

5.3. Alkaline granite and peralkaline granite orthogneiss

In the alkaline orthogneiss (sample MTG-10), 17 analyses were obtained from magmatic areas with oscillatory zoning (Supplementary Table 4), yielding ages between 478 and 452 Ma, with a mean calculated by Squid of 462 ± 3 Ma (MSWD = 1.9, Fig. 7a). This mean is consistent with the field relationships observed between the granodiorite and alkali-granite gneisses and the alkaline gneisses (see Section 2.3). However, it would be difficult to explain the three oldest analyses given the absence of obvious xenocrystic cores or inherited grains. For this reason, and taking into account previous geochronological results (~472 Ma, ID-TIMS U–Pb in zircon, Rodríguez et al., 2007), we favor an interpretation in which the most probable age is closest to the maximum age, while the remaining ages are the result of Pb-loss. Accordingly, we have used the oldest most concordant analyses to obtain a concordia age of 468 ± 2 Ma, with a MSWD of 0.37 (Fig. 7b).

In the peralkaline orthogneiss (sample MTG-6), the amount of inclusions and the metamict character of the zircon make it very difficult to find a suitable place to aim the oxygen beam. Yet, using the high spatial resolution provided by the SHRIMP it was possible to obtain 18 analyses in zircon grains from this sample (Supplementary Table 5). The results are spread continuously between 495 and 456 Ma, with a mean calculated by Squid of 474 ± 4 Ma (MSWD = 13, Fig. 8). As with the alkaline orthogneiss (sample MTG-10), obtaining a reliable age from the SHRIMP data is problematic because the data is spread across 40 m.y., so we must count on additional data. In this case, field relationships between the alkali-granite gneisses and the peralkaline gneisses suggest that the latter is younger than the former, that is, younger than 475 Ma. For this reason, we consider the age of 482 Ma obtained by Montero et al. (2009a) is too old for this peralkaline magmatic event. We prefer the mean calculated for our data (474 ± 4 Ma) because it is more consistent with the field relationships, even though it is statistically flawed.

5.4. Additional data: tonalitic orthogneiss

A preliminary geochronological survey carried out in the A Pioza tonalitic orthogneiss reveals a complex evolution (Castiñeiras et al., in prep.). There are two main zircon types based on the cathodoluminescence textures, one type shows oscillatory zoning, whereas the other exhibits sector zoning. Both varieties are rimmed by dark homogeneous zones. These rims show diffuse boundaries with the inner zone,

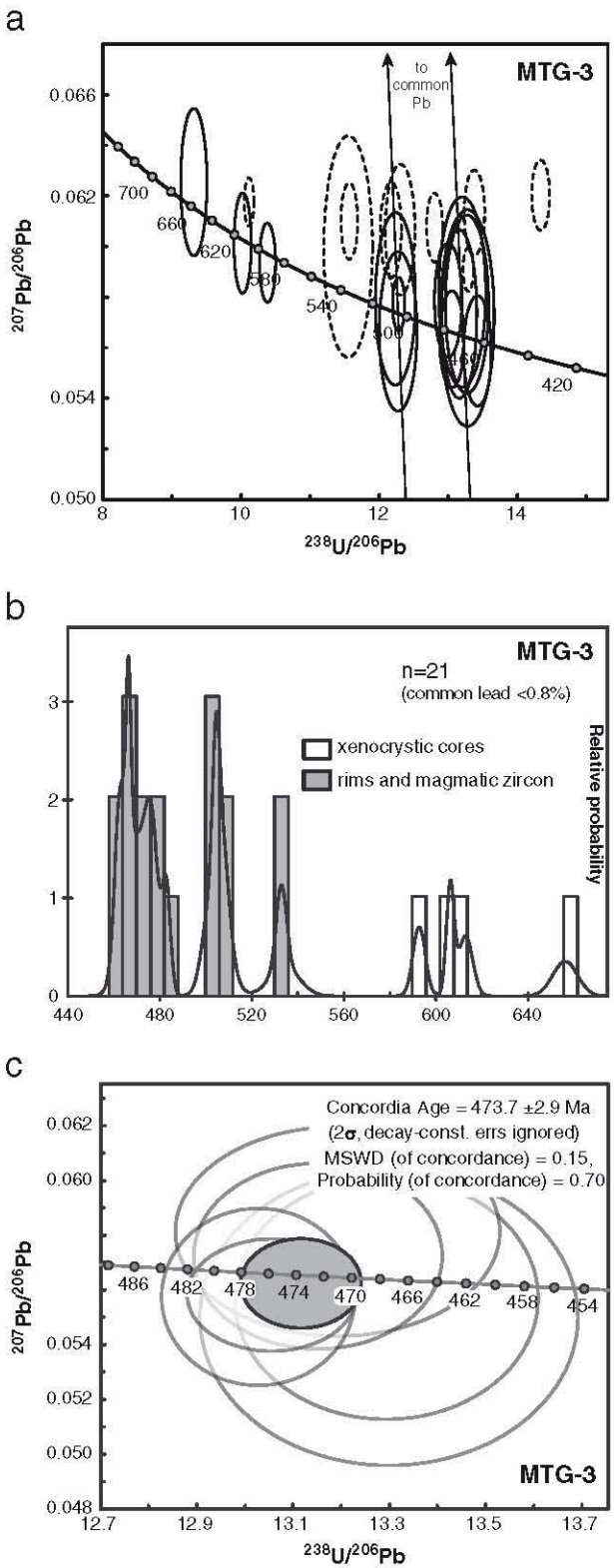

Fig. 5. (a) Tera-Wasserburg plot for sample MTG-3 showing the distribution of zircon analyses with ages younger than 1.0 Ga. Dashed ellipses represent analyses affected by a combination of lead loss and common lead. (b) Relative probability density plot. White bars represent xenocrystic cores, whereas grey bars stand for rims and magmatic zircon. (c) Concordia age (light grey ellipse) obtained from the youngest set of analyses.

suggesting that they were formed by recrystallization. The age record is also complex and not well understood yet. Oscillatory zones yield individual ages ranging from 515 to 487 Ma, with two prominent age

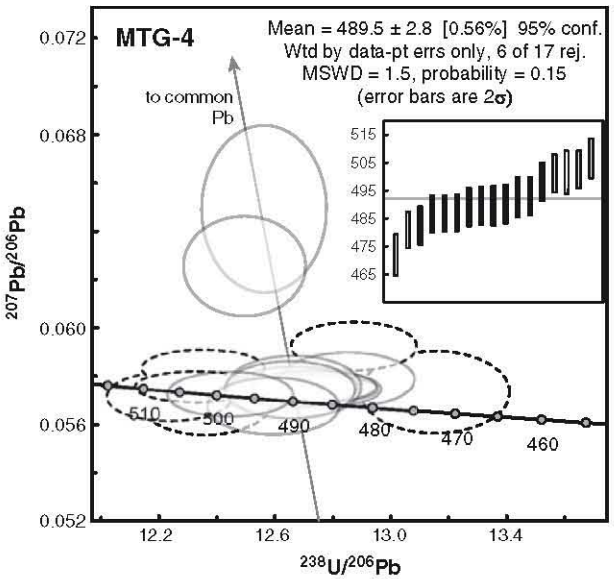

Fig. 6. Tera-Wasserburg plot for sample MTG-4 showing the distribution of zircon analyses. Inset, weighted mean calculated for this sample. White bars and dashed ellipses represent analyses not considered in the calculation of the age.

groups at 513 ± 5 and 491 ± 5 Ma. The ages obtained from sector zones are distributed between 529 and 473 Ma, with at least two age groups at 526 ± 5 and 505 ± 5 Ma. The rims also display a complex age distribution (from 540 to 407), probably due to incomplete isotopic equilibration during recrystallization and/or lead loss. The complexity of the age record and the variety of cathodoluminescence textures are probably the result of a process of magma mixing, also recognized at outcrop scale (Rodríguez Aller, 2005).

6. The age results in the regional framework

The results support the existence of two main magmatic events, confirming the two-step model implied by Abati et al. (2010). However, our work provides new and further refinement. The calc-alkaline association can be divided in two age groups: Cambrian granodiorites and tonalites (490–500 Ma), and Ordovician alkali-granites (470–480 Ma). The latter are slightly older than the alkaline and peralkaline granites (470–475 Ma), but both could be grouped into a single broad Ordovician suite. The age of the alkaline and peralkaline granites places the age of the alkaline mafic dykes that intruded the alkali-granites at 470–475 Ma. However, the age of some sub-alkaline mafic lenses is 490–500 Ma (Abati et al., 2010).

The data obtained from the alkali-granite samples (MTG-3 and MTG-4) can be interpreted in a different way. Assuming that the youngest ages are the result of lead loss, which is difficult to assess in SIMS analyses, the Cambrian ages (around 505 Ma) could be regarded as the actual crystallization age of these plutonic massifs. However, field data and previous work have not considered crustal recycling processes when dealing with Lower Paleozoic magmatism (e.g. Bea et al., 2007). Therefore the youngest concordant U–Pb zircon population is more suitable for dating their crystallization age. Our data suggest that the Cambrian input was inherited from the granite source and/or assimilated from the host. Both processes may provide statistically older crystallization ages (e.g. Abati et al., 2010). The Cambrian input in samples MTG-3 and MTG-4 cannot be explained by assimilation from the host, since the host sedimentary sequence is Neoproterozoic (ca. 560 Ma; Díez Fernández et al., 2010), and the samples were collected far from the Cambrian massifs and lack enclaves. According to their age spectra, the alkali-granites can be interpreted as the result of recycling during the Ordovician (470–480 Ma) of a Neoproterozoic/Cadomian basement (560–600 Ma

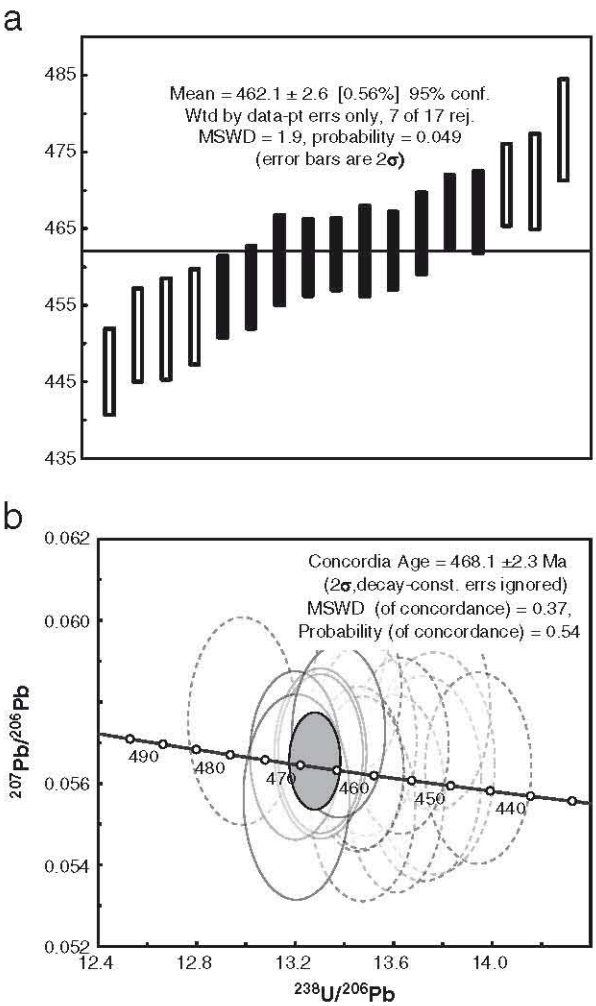

Fig. 7. (a) Weighted average calculated by Squid from all the analyses of sample MTG-10. White bars represent analyses not considered in the calculation of the age. (b) Tera-Wasserburg plot for sample MTG-10 showing the concordia age (light grey ellipse) calculated for this sample using the oldest set of analyses. See text for explanation.

input) that had previously been intruded by Cambrian granitoids (490–500 Ma input). The geochemistry of the Ordovician granites would be a legacy from their protoliths (mostly greywackes and granodiorites; e.g. Klimas-August, 1990; Floyd et al., 2000).

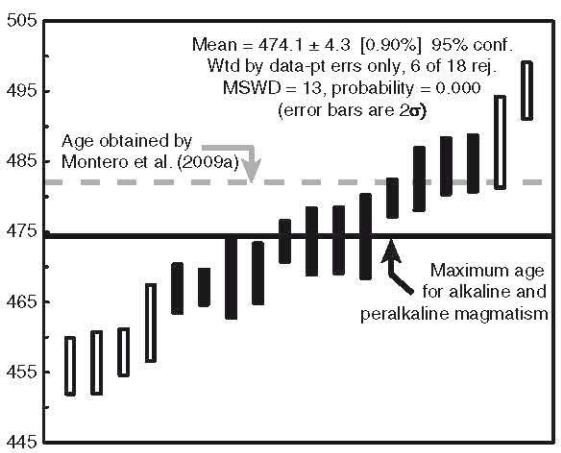

Fig. 8. Weighted average plot showing the complex age distribution for sample MTG-6. See text for explanation.

The alkaline association shows a stronger mantle influence than the Ordovician alkali-granites of the calc-alkaline association (Pin et al., 1992; Rodríguez Aller, 2005; Montero et al., 2009a). The time interval and similar paleogeographic position in which both the alkaline and youngest members of the calc-alkaline association occur suggest that the latter are also related to Ordovician continental rifting, as is widely accepted for the alkaline/peralkaline association. Such correlation and both the geochemical and geochronological data suggest that the role of the mantle gained importance through time during the rifting process.

The Cambrian event (490–500 Ma) can be tentatively linked to the building of a continental-arc system at the Gondwana periphery (Abati et al., 2010; Díez Fernández et al., 2010). The activity of this system likely started during the Lower Cambrian (515–525 Ma; Arenas et al., 2009), as also reported by the preliminary results from the tonalitic orthogneisses. The inherited input of the granodiorites (Fig. 4a and b) may reflect assimilation from the sedimentary host, but arc-related recycling cannot be ruled out.

"Calc-alkaline" affinities occur in both the Ordovician rifting and the Cambrian volcanic-arc systems. So the link between geochemical signature and geodynamic setting is not definitive. This point is also a long-standing controversy in the autochthonous pre-Variscan sequences, where intraplate alkaline-calcic to calc-alkaline magmatism spanning the range of 470–490 Ma occurs in the so-called Ollo de Sapo Domain and its correlatives (Fig. 1b; Valverde-Vaquero and Dunning, 2000; Bea et al., 2006; Solá et al., 2008; Montero et al., 2009b; Díez Montes et al., 2010). In the absence of significant coeval deformation, the calk-alkaline magmatism occurring there may well be linked to other orogenic processes, and the volcanic-arc option can be discarded in light of its paleogeographical position. Díez Montes et al. (2010) placed such igneous activity in a siliceous province (*sensu* Bryan et al., 2002), which would have been thermally fed by mafic magmas that underplated the lower crust (Bea et al., 2007). A similar petrogenetic model was suggested to explain the peraluminous/peralkaline duality of the Cambro-Ordovician magmatism in the external sections of the continental margin (Montero et al., 2009b). Taking this and our data into account, the arrival of mantle-derived material and the heating of the middle and upper crust in the Ordovician affected most of the Gondwana continental margin during a relatively short time period (470–480 Ma). Such a scenario would involve a large-scale thermal anomaly that extended hundreds of kilometres across the crust-mantle boundary and lower crust. This favored crustal melting and thus widespread complex magmatism, likely coupled with extensional activity. High subsidence rates in the continental platform were accompanied by block tilting and erosion of pre-Ordovician sequences. Both processes shaped the upper crust to host the wide and shallow Armorican marine platform in the Early–Middle Ordovician (e.g. von Raumer et al., 2006), before igneous activity had ceased (Gutiérrez-Alonso et al., 2007).

7. A Lower Paleozoic convection system

The major magmatic events affecting the NW Iberian margin of Gondwana during the Lower Paleozoic can be explained by the interaction between a mantle convection system and an Ordovician injection of hot asthenosphere, both of them connected to a single subduction system (Fig. 9).

The classical model including dehydration reactions in a down-going oceanic crust and melting of the overriding mantle (e.g. Ulmer, 2001) provides an explanation for the Cambrian magmatism in the most external margin of Gondwana, which likely took place in a continental-arc setting (Fig. 9a). Slab-pull forces in a steep subduction setting likely produced significant back-arc extension until ocean ridge incision (Fig. 9b). These forces could have also promoted crustal necking of continental sections outside the arc, thus favoring coeval intraplate Cambrian volcanism (Díez Montes et al., 2010). In addition,

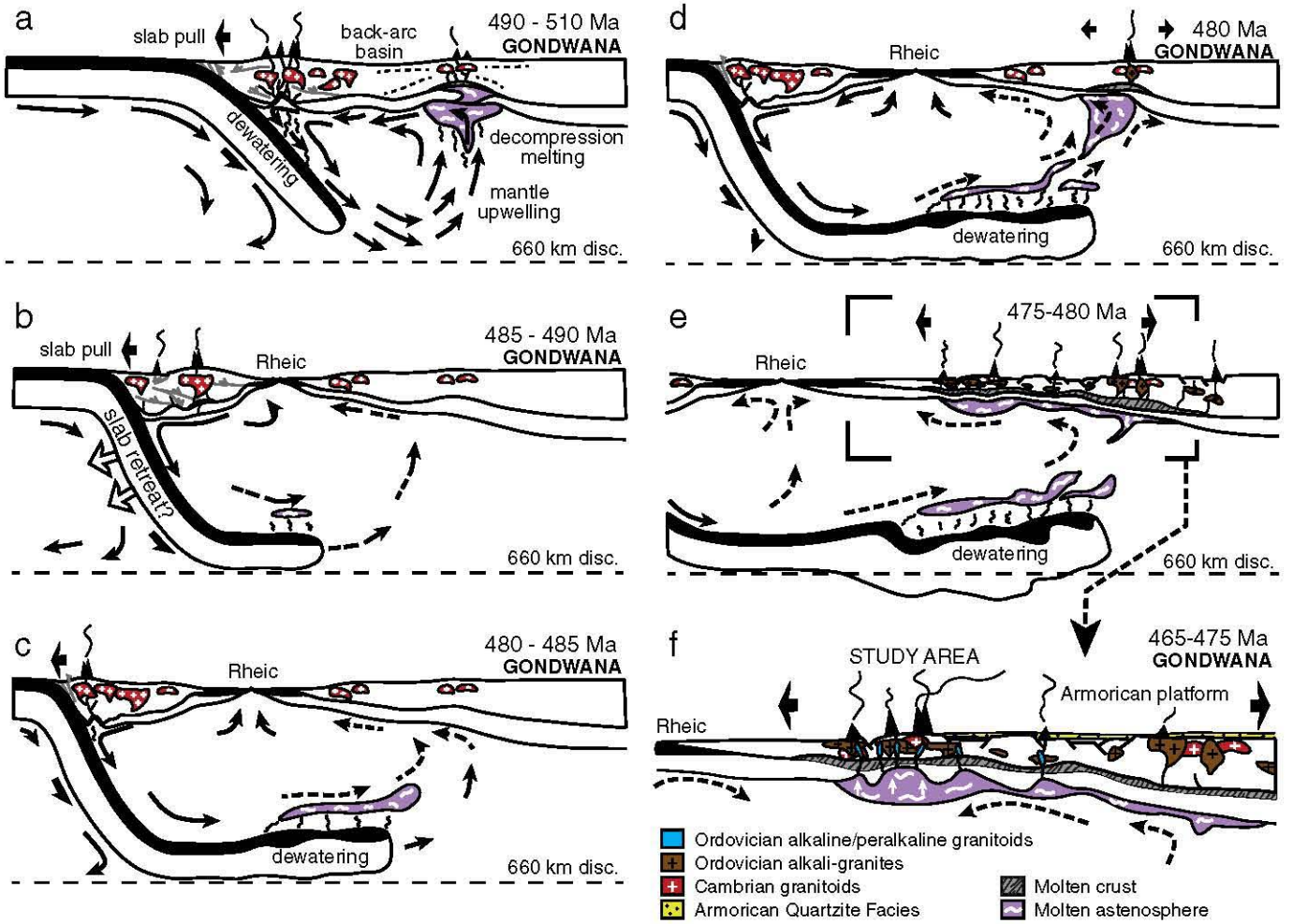

Fig. 9. Geodynamic evolution of the Iberian Gondwana margin during the Lower Paleozoic. (a) Building of a continental volcanic arc and development of off-axis intraplate magmatism fed by crust necking and mantle upwelling (Ollo de Sapo Fm.). Strong convective flow. (b) Opening of the Rheic Ocean and establishment of a main spreading centre in the back-arc basin (ridge incision?). Weak convective flow. (c) Drifting of the peri-Gondwanan arc system and growing of an asthenospheric mantle plume along the 660 km discontinuity. (d) Injection of the asthenospheric mantle plume. Beginning of the major Ordovician magmatic event in the continental margin (Ollo de Sapo and correlatives). (e) Spreading of the asthenospheric mantle plume beneath the Gondwanan lithosphere and extensive crust melting. (f). Arrival of mantle fluids in the external sections of the margin (over-pressure beneath the crust?). Mixing of mantle- and crust-derived melts (alkaline/peralkaline magmatism). Establishment of a wide and shallow marine platform.

the downwelling of cold material into the mantle could have also generated focused, sub-lithospheric, mantle upwellings (Conrad et al., 2010; Faccenna et al., 2010) that, coupled with decompression melting, may have fed this off-axis igneous activity (Raddick et al., 2002).

Flat subduction may hydrate laterally extensive regions of continental lithosphere, feeding intraplate magmatism and extension far inboard of the arc–trench (Sommer and Gauert, 2011). Stress coupling of the upper plate with a flat slab also causes compression in the back-arc sections (Cross and Pilger, 1982). Such processes weaken the slab-pull forces that might have favored back-arc extension, making it difficult to harmonize a Cambrian flat subduction system beneath Gondwana with the sea-floor spreading and terrane drifting developed in NW Iberia.

Steep subduction of oceanic lithosphere triggers return/corner flow in the mantle (Sleep and Toksöz, 1971; Toksöz and Hsui, 1978). The drifting of continental volcanic-arc systems may be also driven by shear tractions exerted on their base by viscous coupling to convective mantle flow (Fig. 9; Conrad and Lithgow-Bertelloni, 2002). The highest rates of extension related to this flow are expected during the transient stage of slab descent into the upper mantle, fading away after the interaction of the slab with the 660 km discontinuity (Faccenna et al., 2010). In our case, this period in particular can be placed in the interval 495–525 Ma, from the built-up of the Cambrian peri-Gondwanan arc to the birth of the Rheic Ocean (Fig. 9b), although the subduction of a mid-ocean ridge (Nance et al., 2002) or slab retreat (e.g. the Mediterranean basins; Jolivet et al., 2008) may have also accelerated the widening of the back-arc, and may have activated extensional dynamics within the arc edifice (e.g. Castiñeiras et al., 2010). Large-scale convective flow related to subduction implies a regional tensional setting across the continental margin as long as subduction continues. The consumption of Iapetan lithosphere was largely completed by Silurian times (Pollock et al., 2007), but might account for most of the pre-Silurian extensional dynamics in the Gondwana margin. Given that the strength of the convective flow beneath Gondwana would decrease as the arc–trench migrated towards Laurussia, an alternative source of tensional forces is necessary to explain the subsequent Ordovician intracontinental rifting.

The Ordovician magmatism affected most of the external margin of Gondwana, from the sections intruded by intraplate volcanism to the edge of the continent, in a relatively short time period (see Section 6). Geochemical and geochronological data suggest that the Ordovician thermal event was coupled with an increasing role of the mantle in the geochemistry of coeval magmatism. The mantle fingerprint was different across the Gondwana margin. In the sections located towards the mainland, which were likely affected by moderate

extension during the Cambrian (Fig. 9b), the mantle exerted limited geochemical influence (Montero et al., 2009b; Díez Montes et al., 2010), but associated heat fed a thermal anomaly that caused significant crust melting (intraplate magmatism). On the other hand, the external sections of the margin would have undergone significant Cambrian crustal thinning, being prone to host both heat and mantle-derived fluids at shallow levels (alkaline/peralkaline magmatism) that would have respectively triggered significant crust melting (Ordovician alkali-granites) and produced mantle–crust mixing (peraluminous/peralkaline duality; Montero et al., 2009a).

High temperatures in the shallow back-arc mantle are a characteristic feature of steep subduction zones (Currie and Hyndman, 2006). Both protracted extension and thinning of the lithosphere, and an incursion of heat and/or hot asthenosphere material would explain the increasing mantle influence. There are arguments supporting both processes. Lower Paleozoic subduction beneath Gondwana provided long-lived but weak extension landwards and, at the same time, could have fed a megalith (Ringwood and Irifune, 1988) floating and straddling the discontinuity at the 660 km boundary (Fig. 9c). Megaliths grow with time and can feed mantle plumes and/or upwellings (e.g. Yamamoto and Hoang, 2009; Faccenna et al., 2010). Mantle–plume activity has been previously proposed to explain the Cambro-Ordovician magmatism (Pin and Marini, 1993), and is also identified as one of the main mechanism triggering back-arc extension (e.g. the Sea of Japan; Nohda et al., 1988; Zhao et al., 2007). However, the paleogeographical distribution of such activity across the margin cannot be explained by vertical plume ascent alone, which would have created a single and fixed hotspot. Progressive dehydration of the stagnant slab could have induced melting across the back-arc asthenosphere, and fed a plume at shallower levels. Significant water release may also occur several hundred kilometres inboard of the trench (van der Lee et al., 2008; Sommer and Gauert, 2011). This process not only provides an additional source of intraplate magmas, but can also supercharge a pre-existing plume and accelerate its ascent (Fig. 9d). A coeval subduction-related convecting system could transform their initial vertical flow into an oceanward current beneath the subcontinental lithosphere. The wedge morphology of the rifted continental crust would have favored such a current as well. The thermal component of this current would have affected the rheology of the overlying crust, favoring further extension and the Ordovician intracontinental rifting (Fig. 9e and f; e.g. the Sea of Japan; Tatsumi et al., 1990; Zhao et al., 2007). Mantle upwelling would have been accompanied by inland topographic uplift (e.g. Rohrman et al., 2002), while the erosion of local exposures of the previous sedimentary sequences would produce an Ordovician unconformity (Fig. 9f).

The injection of asthenospheric material would have also affected the subcontinental lithosphere composition. Sm/Nd data from Ordovician mafic rocks suggest they were extracted from a heterogeneous subcontinental lithosphere, including a mantle that was enriched at about 0.9–1.1 Ga (Murphy et al., 2008). This might be a hint on the incursion of previously subducted older material, since the long-lived Avalonian/Cadomian subduction system may have fed an asthenospheric reservoir with Early Neoproterozoic and Mesoproterozoic rocks (e.g. Murphy et al., 2009). The traces of these rocks still represent a major enigma in the Variscan belt because they are hidden (covered?), were eroded, and/or consumed in former subduction systems. Yet there is some evidence left (Sánchez Martínez et al., 2011), and some sedimentary sequences in NW Iberia contain ancient exposures (Gutiérrez-Alonso et al., 2005). In addition, relicts of Early Neoproterozoic arc-related rocks can be found along the Pan-African Hoggar megasuture (Abdelsalam et al., 2002; Cordani et al., 2003; Bea et al., 2009), and in the sedimentary cover of northern Gondwana, both in its eastern (Avigad et al., 2003; Avigad et al., 2007; Morag et al., 2011) and central sections (Avigad et al., in press). These domains broaden the paleoposition recently given to NW Iberia during the Late Neoproteozoic (Díez Fernández et al., 2010) and Lower Paleozoic (Bea et al., 2010; Díez Fernández et al., 2010). Thus we speculate that the evidence of a former Mesoproterozoic geological history in northern Gondwana could have been pumped from deep-seated mantle reservoirs in a Cambro-Ordovician convection system, and coevally dismantled and spread over its basement during the transition from active to passive margin conditions.

8. Conclusions

U–Pb zircon dating of the main suites of igneous rocks that intruded the most external margin of Gondwana during the Lower Paleozoic reveals the existence of two magmatic pulses in NW Iberia, dated at 489 ± 4 Ma (granodiorites) and 474 ± 3 Ma (alkali-granites), and a younger alkaline pulse, dated at ca. 470–475 Ma (alkaline and peralkaline granites). The timing of the magmatism, combined with the analysis of its paleogeographical distribution, can be explained by major lithosphere-scale processes related to the interplay between protracted subduction, mantle rheology and asthenosphere dynamics.

The Cambrian magmatism developed in a continental-arc setting, while coeval intraplate igneous activity affected more internal sections of the continent. Back-arc extension, sea-floor broadening and terrane drifting gave birth to the Rheic Ocean. These processes were mostly controlled by slab-pull forces related to steep subduction. Coeval mantle upwelling and shear traction exerted on the subcontinental lithosphere by viscous coupling to subduction-related convective mantle flow may have also contributed. However, its role, particularly that of the convective flow, likely gained importance during the widening of the back-arc, compared to slab-pull. The stagnation and progressive dehydration of the previously subducted lithosphere along the 660 km discontinuity fed an asthenospheric mantle plume, whose incursion occurred in Ordovician times. The interaction of this plume with the subduction-related convection cell created an oceanward hot subcontinental current that triggered intracontinental rifting, crustal recycling and extensive magmatism that affected the external margin of Gondwana.

Acknowledgements

The authors are grateful to Jürgen von Raumer and an anonymous reviewer for their critical reading and encouraging advice. Damian Nance is thanked for his editorial work and suggestions. This work has been funded by research projects CGL2007-65338-C02-01 and -02/BTE of the Dirección General de Programas y Transferencia del Conocimiento (Spanish Ministry of Science and Innovation). P. Castiñeiras' stay at the SUMAC facility was financed with a "Profesores UCM en el extranjero" and a "José Castillejo" travel aids. J. Gómez Barreiro appreciates financial support from the Spanish Ministry of Science and Innovation through the Ramon y Cajal program (RYC-2010-05818).

Appendix A. Supplementary data

Supplementary data associated with this article can be found in the online version, at doi:10.1016/j.gr.2011.07.028. These data include Google maps of the most important areas described in this article.

References

Abati, J., Dunning, G.R., Arenas, R., Díaz García, F., González Cuadra, P., Martínez Catalán, J.R., Andonaegui, P., 1999. Early Ordovician orogenic event in Galicia (NW Spain): evidence from U–Pb ages in the uppermost unit of the Ordenes Complex. Earth and Planetary Science Letters 165 (2), 213–228.

Abati, J., Gerdes, A., Fernández-Suárez, J., Arenas, R., Whitehouse, M.J., Díez Fernández, R., 2010. Magmatism and early-Variscan continental subduction in the northern Gondwana margin recorded in zircons from the basal units of Galicia, NW Spain. Geological Society of America Bulletin 122 (1–2), 219–235.

Abdelsalam, M.G., Liégeois, J.P., Stern, R.J., 2002. The Saharan metacraton. Journal of African Earth Sciences 34 (3–4), 119–136.

Ancochea, E., Arenas, R., Brandle, J.L., Peinado, M., Sagredo, J., 1988. Caracterización de las rocas metavolcánicas silúricas del NO del Macizo Ibérico. Geociencias, Aveiro 3, 23–34.

Andonaegui, P., González del Tánago, J., Arenas, R., Abati, J., Martínez Catalán, J.R., Peinado, M., Díaz García, F., 2002. Tectonic setting of the Monte Castelo gabbro (Ordenes Complex, northwestern Iberian Massif): evidence for an arc-related terrane in the hanging wall to the Variscan suture. In: Martínez Catalán, J.R., Hatcher, R.D., Arenas, R., Díaz García, F. (Eds.), Variscan–Appalachian dynamics: the building of the late Paleozoic basement: Geological Society of America Special Paper, pp. 37–56.

Arenas, R., 1984. Características y significado del volcanismo ordovícico-silúrico de la serie autóctona envolvente del Macizo de Cabo Ortegal (Galicia, NW de España): Revista de Materiales y Procesos Geológicos, II, pp. 135–144.

Arenas, R., 1988. Evolución petrológica y geoquímica de la unidad alóctona inferior del complejo metamórfico básico-ultrabásico de Cabo Ortegal (Unidad de Moeche) y del Silúrico parautóctono, Cadena Hercínica Ibérica (NW de España). Corpus Geologicum Gallaecia 4, 1–543.

Arenas, R., Martínez Catalán, J.R., Sánchez Martínez, S., Fernández-Suárez, J., Andonaegui, P., Pearce, J.A., Corfú, F., 2007. The Vila de Cruces ophiolite: a remnant of the early Rheic Ocean in the Variscan suture of Galicia (northwest Iberian Massif). Journal of Geology 115 (2), 129–148.

Arenas, R., Sánchez Martínez, S., Castineiras, P., Jeffries, T.E., Díez Fernández, R., Andonaegui, P., 2009. The basal tectonic melange of the Cabo Ortegal Complex (NW Iberian Massif): a key unit in the suture of Pangea. Journal of Iberian Geology 35 (2), 85–125.

Arps, C.E.S., 1970. Petrology of a part of the Western Galicia Basement between the río Jallas and the Ría de Arosa (NW Spain) with emphasis on zircon investigations. Leidse Geologische Mededelingen 46, 57–155.

Avigad, D., Kolodner, K., McWilliams, M., Persing, H., Weissbrod, T., 2003. Origin of northern Gondwana Cambrian sandstone revealed by detrital zircon SHRIMP dating. Geology 31 (3), 227–230.

Avigad, D., Stern, R.J., Beyth, M., Miller, N., McWilliams, M.O., 2007. Detrital zircon U–Pb geochronology of Cryogenian diamictites and Lower Paleozoic sandstone in Ethiopia (Tigrai): age constraints on Neoproterozoic glaciation and crustal evolution of the southern Arabian–Nubian Shield. Precambrian Research 154 (1–2), 88–106.

Avigad, D., Gerdes, A., Morag, N. and Bechstädt, T., in press. Coupled U–Pb–Hf of detrital zircons of Cambrian sandstones from Morocco and Sardinia: Implications for provenance and Precambrian crustal evolution of North Africa. Gondwana Research. Accepted Manuscript. doi:10.1016/j.gr.2011.06.005.

Ballèvre, M., Bosse, V., Ducassou, C., Pitra, P., 2009. Palaeozoic history of the Armorican Massif: models for the tectonic evolution of the suture zones. Comptes Rendus Geosciences 341 (2–3), 174–201.

Barrera, J.L., Farias, P., González Lodeiro, F., Marquínez García, J., Martín Parra, L.M., Martínez Catalán, J.R., del Olmo Sanz, A. and de Pablo Maciá, J.G., 1989. Mapa y memoria de la Hoja nº 17–27 (Orense-Verín) del Mapa Geológico de España, Escala 1/200.000. Instituto Geológico y Minero de España.

Bea, F., Montero, P., Talavera, C., Zinger, T., 2006. A revised Ordovician age for the Miranda do Douro orthogneiss, Portugal. Zircon U–Pb ion-microprobe and LA-ICPMS dating. Geologica Acta 4, 395–401.

Bea, F., Montero, P., Gonzalez Lodeiro, F., Talavera, C., 2007. Zircon inheritance reveals exceptionally fast crustal magma generation processes in central iberia during the cambro-ordovician. Journal of Petrology 48, 2327–2339.

Bea, F., Abu-Anbar, M., Montero, P., Peres, P., Talavera, C., 2009. The similar to 844 Ma Moneiga quartz-diorites of the Sinai, Egypt: evidence for Andean-type arc or rift-related magmatism in the Arabian–Nubian Shield? Precambrian Research 175 (1–4), 161–168.

Bea, F., Montero, P., Talavera, C., Abu Anbar, M., Scarrow, J.H., Molina, J.F., Moreno, J.A., 2010. The palaeogeographic position of Central Iberia in Gondwana during the Ordovician: evidence from zircon chronology and Nd isotopes. Terra Nova 22, 341–346.

Black, L.P., Kamo, S.L., Allen, C.M., Davis, D.W., Aleinikoff, J.N., Valley, J.W., Mundil, R., Campbell, I.H., Korsch, R.J., Williams, I.S., Foudoulis, C., 2004. Improved 206Pb/238U microprobe geochronology by the monitoring of a trace-element-related matrix effect, SHRIMP, ID-TIMS, ELA-ICP-MS and oxygen isotope documentation for a series of zircon standards. Chemical Geology 205, 115–140.

Bryan, S.E., Riley, T.R., Jerram, D.A., Stephens, C.J., Leat, P.T., 2002. Silicic volcanism: an undervalued component of large igneous provinces and volcanic rifted margins. Geological Society of America Special Paper, 362, pp. 97–118.

Castiñeiras, P., Navidad, M., Liesa, M., Carreras, J., Casas, J.M., 2008. U–Pb zircon ages (SHRIMP) for Cadomian and Early Ordovician magmatism in the Eastern Pyrenees: new insights into the pre-Variscan evolution of the northern Gondwana margin. Tectonophysics 461 (1–4), 228–239.

Castiñeiras, P., Díaz García, F., Gómez Barreiro, J., 2010. REE-assisted U–Pb zircon age (SHRIMP) of an anatectic granodiorite: constraints on the evolution of the A Silva granodiorite, Iberian allochthonous complexes. Lithos 116 (1–2), 153–166.

Conrad, C.P., Lithgow-Bertelloni, C., 2002. How mantle slabs drive plate tectonics. Science 298, 207–209.

Conrad, C.P., Wu, B., Smith, E.I., Bianco, T.A., Tibbetts, A., 2010. Shear-driven upwelling induced by lateral viscosity variations and asthenospheric shear: a mechanism for intraplate volcanism. Physics of the Earth and Planetary Interiors 178 (3–4), 162–175.

Cordani, U.G., Brito-Neves, B.B., D'Agrella, M.S., 2003. From Rodinia to Gondwana: a review of the available evidence from South America. Gondwana Research 6 (2), 275–283.

Cross, T.A., Pilger, R.H., 1982. Controls of subduction geometry, location of magmatic arcs, and tectonics of arc and back-arc regions. Geological Society of America Bulletin 93, 545–562.

Crowley, Q.G., Floyd, P.A., Winchester, J.A., Franke, W., Holland, J.G., 2000. Early Palaeozoic rift-related magmatism in Variscan Europe: fragmentation of the Armorican Terrane Assemblage. Terra Nova 12 (4), 171–180.

Currie, C.A., Hyndman, R.D., 2006. The thermal structure of subduction zone back arcs. Journal of Geophysical Research-Solid Earth 111 (B8), B08404.

Díez Balda, M.A., Vegas, R., González Lodeiro, F., 1990. Central-Iberian Zone. Autochthonous Sequences. Structure. In: Dallmeyer, R.D., Martínez García, E. (Eds.), Pre-Mesozoic Geology of Iberia. Springer-Verlag, Berlín, pp. 172–188.

Díez Fernández, R., Martínez Catalán, J.R., 2009. 3D Analysis of an Ordovician igneous ensemble: a complex magmatic structure hidden in a polydeformed allochthonous Variscan unit. Journal of Structural Geology 31 (3), 222–236.

Díez Fernández, R., Martínez Catalán, J.R., Gerdes, A., Abati, J., Arenas, R., Fernández-Suárez, J., 2010. U–Pb ages of detrital zircons from the Basal allochthonous units of NW Iberia: provenance and paleoposition on the northern margin of Gondwana during the Neoproterozoic and Paleozoic. Gondwana Research 18 (2–3), 385–399.

Díez Fernández, R., Martínez Catalán, J.R., Arenas Martín, R., Abati Gómez, J., 2011. Tectonic evolution of a continental subduction–exhumation channel: Variscan structure of the basal allochthonous units in NW Spain. Tectonics 30 (3), TC3009.

Díez Fernández, R., Martínez Catalán, J.R., Gómez Barreiro, J. and Arenas, R., accepted for publication. Extensional flow during gravitational collapse: a tool for setting plate convergence (Padrón migmatitic dome, Variscan belt, NW Iberia). The Journal of Geology.

Díez Montes, A., Martínez Catalán, J.R., Bellido Mulas, F., 2010. Role of the Ollo de Sapo massive felsic volcanism of NW Iberia in the Early Ordovician dynamics of northern Gondwana. Gondwana Research 17 (2–3), 363–376.

Dörr, W., Fiala, J., Vejnar, Z., Zulauf, G., 1998. U–Pb zircon ages and structural development of metagranitoids of the Teplá crystalline complex: evidence for pervasive Cambrian plutonism within the Bohemian massif (Czech Republic). Geologische Rundschau 87, 135–149.

Eguiluz, L., Gil Ibarguchi, J.I., Abalos, B., Apraiz, A., 2000. Superposed Hercynian and Cadomian orogenic cycles in the Ossa-Morena zone and related areas of the Iberian Massif. Geological Society of America Bulletin 112 (9), 1398–1413.

Faccenna, C., Becker, T.W., Lallemand, S., Lagabrielle, Y., Funiciello, F., Piromallo, C., 2010. Subduction-triggered magmatic pulses: a new class of plumes? Earth and Planetary Science Letters 299 (1–2), 54–68.

Farias, P., Gallastegui, G., González Lodeiro, F., Marquínez García, J., Martín-Parra, L.M., Martínez Catalán, J.R., Pablo Maciá, J.G.d., Rodríguez-Fernández, L.R., 1987. Aportaciones al conocimiento de la litoestratigrafía y estructura de Galicia Central: Mem. Museo e Lab. Miner. Geol., Fac. Ciencias, Univ. Porto, 1, pp. 411–431.

Ferragne, A., 1972. Le Précambrien et le Paléozoïque de la province d'Orense (Nord-ouest de l'Espagne). Stratigraphie-tectonique-métamorphisme. PhD Thesis, University of Bordeaux, Bordeaux, 249 pp.

Floor, P., 1966. Petrology of an aegirine–ribeckite gneiss-bearing part of the Hesperian Massif: the Galiñeiro and surrounding areas, Vigo, Spain. Leidse Geologische Mededelingen 36, 204.

Floyd, P.A., Winchester, J.A., Seston, R., Kryza, R., Crowley, Q.G., 2000. Review of geochemical variation in Lower Palaeozoic metabasites from the NE Bohemian Massif: intracratonic rifting and plume–ridge interaction. In: Franke, W., Haak, V., Oncken, O., Tanner, D. (Eds.), Orogenic processes: quantification and modelling in the Variscan Belt: Geological Society, London, Special Publications, pp. 155–174.

Franke, W., 1995. Stratigraphy, structure, and igneous activity. In: Dallmeyer, R.D., Franke, W., Weber, K. (Eds.), Pre-Permian Geology of Central and Eastern Europe. Springer, pp. 277–294.

Franke, W., 2000. The mid-European segment of the Variscides: tectonostratigraphic units, terrane boundaries and plate tectonic evolution. In: Franke, W., Haak, V., Oncken, O., Tanner, D. (Eds.), Orogenic processes: quantification and modelling in the Variscan Belt: Geological Society, London, Special Publication, pp. 35–61.

Fuenlabrada, J.M., Arenas, R., Sánchez Martínez, S., Díaz García, F., Castiñeiras, P., 2010. A peri-Gondwanan arc in NW Iberia: I: isotopic and geochemical constraints on the origin of the arc—a sedimentary approach. Gondwana Research 17 (2–3), 338–351.

Furnes, H., Kryza, R., Muszynski, A., 1989. Geology and geochemistry of Early Paleozoic volcanics of the Swierzawa Unit, Kaczawa Mts, W. Sudetes, Poland. Neues Jahrbuch für Geologie und Paläontologie, Monatshefte H3, 136–154.

Gallastegui, G., Martín Parra, L.M., de Pablo Maciá, J.G., Rodríguez-Fernández, L.R., 1987. Las metavulcanitas del Dominio Esquistoso de Galicia-Tras-os.Montes: petrografía, geoquímica y ambiente geotectónico (Galicia, NO de España): Cuadernos do Laboratorio Xeolóxico de Laxe, 12, pp. 127–139.

García Garzón, J., Pablo Maciá, J.G.d., Llamas Borrajo, J.F., 1981. Edades absolutas obtenidas mediante el método Rb-Sr de dos cuerpos de ortogneises en Galicia Occidental. Boletín Geológico Minero 92, 443–455.

Gómez Barreiro, J., Martínez Catalán, J.R., Arenas, R., Castiñeiras, P., Abati, J., Díaz García, F., Wijbrans, J.R., 2007. Tectonic evolution of the upper allochthon of the Órdenes Complex (northwestern Iberian Massif): structural constraints to a polyorogenic peri-Gondwanan terrane. In: Linnemann, U., Nance, R.D., Kraft, P., Zulauf, G. (Eds.), The evolution of the Rheic Ocean: from Avalonian–Cadomian active margin to Alleghenian–Variscan collision: Geological Society of America Special Paper, 423, pp. 315–332.

Gómez Barreiro, J., Martínez Catalán, J.R., Díez Fernández, R., Arenas, R., Díaz García, F., 2010. Upper crust reworking during gravitational collapse: the Bembibre-Pico Sacro detachment system (NW Iberia). Journal of the Geological Society 167 (4), 769–784.

Gutiérrez-Alonso, G., Fernández-Suárez, J., Collins, A.S., Abad, I., Nieto, F., 2005. Amazonian mesoproterozoic basement in the core of the ibero-Armorican Arc: $^{40}Ar/^{39}Ar$ detrital mica ages complement the zircon's tale. Geology 33 (8), 637–640.

Gutiérrez-Alonso, G., Fernández-Suárez, J., Carlos Gutiérrez-Marco, J., Corfu, F., Murphy, J.B., Suárez, M., 2007. U–Pb depositional age for the upper Barrios Formation (Armorican Quartzite facies) in the Cantabrian zone of Iberia: implications for stratigraphic correlation and paleogeography. Geological Society of America Special Papers, 423, pp. 287–296.

Ireland, T.R., Williams, I.S., 2003. Considerations in zircon geochronology by SIMS. In: H. J.M., Hoskin, P.W.O. (Eds.), zircon. : Reviews in Mineralogy and Geochemistry. Mineralogical Society of America, Washington, pp. 215–241.

Jolivet, L., Augier, R., Faccenna, C., Negro, F., Rimmele, G., Agard, P., Robin, C., Rossetti, F., Crespo-Blanc, A., 2008. Subduction, convergence and the mode of backarc extension in the Mediterranean region. Bulletin de la Societe Geologique de France 179 (6), 525–550.

Kemnitz, H., Romer, R.L., Oncken, O., 2002. Gondwana break-up and the northern margin of the Saxothuringian belt (Variscides of Central Europe). International Journal of Earth Sciences 91, 246–259.

Klimas-August, K., 1990. Genesis of gneisses and granites from the eastern part of the Izera metamorphic complex in the light of studies on zircons from selected geological profiles. Geologia Sudetica 24, 1–71.

Kryza, R., Pin, C., 2010. The Central-Sudetic ophiolites (SW Poland): petrogenetic issues, geochronology and palaeotectonic implications. Gondwana Research 17 (2–3), 292–305.

Liesa, M., Carreras, J., Castineiras, P., Casas, J.M., Navidad, M., Vilá, M., 2011. U–Pb zircon age of Ordovician magmatism in the Albera Massif (Eastern Pyrenees). Geologica Acta 9 (1), 93–101.

Linnemann, U., Gerdes, A., Drost, K., Buschmann, B., 2007. The continuum between Cadomian orogenesis and opening of the Rheic Ocean: constraints from LA-ICP-MS U–Pb zircon dating and analysis of plate-tectonic setting (Saxo-Thuringian zone, northeastern Bohemian Massif, Germany). Geological Society of America Special Paper, 423, pp. 61–96.

Ludwig, K.R., 2002. SQUID 1.02, a user's manual: Berkeley Geochronology Center Special Publication, 2, pp. 1–17.

Ludwig, K.R., 2003. User's manual for Isoplot 3.00. A geochronological Toolkit for Microsoft Excel: Berkeley Geochronology Center, Special Publication, 4, pp. 1–70.

Marquínez García, J.L., 1984. La geología del área esquistosa de Galicia Central (Cordillera Herciniana, NW de España). Memorias del Instituto Geológico y Minero de España 100, 231.

Martínez Catalán, J.R., 2011. Are the oroclines of the Variscan belt related to late Variscan strike-slip tectonics? Terra Nova 1–7.

Martínez Catalán, J.R., Arenas, R., Díaz García, F., Abati, J., 1999. Allochthonous units in the Variscan belt of NW Iberia—terranes and accretionary history. Basement Tectonics 13 (7), 65–84.

Martínez Catalán, J.R., Díaz García, F., Arenas, R., Abati, J., Castineiras, P., González Cuadra, P., Gómez Barreiro, J., Rubio Pascual, F.J., 2002. Thrust and detachment systems in the Ordenes Complex (northwestern Spain): implications for the Variscan–Appalachian geodynamics. In: Martínez Catalán, J.R., Hatcher, R.D., Arenas, R., Díaz García, F. (Eds.), Variscan–Appalachian dynamics: the building of the Late Paleozoic basement: Geological Society of America Special Paper, pp. 163–182.

Martínez Catalán, J.R., Arenas, R., Díaz García, F., Gómez Barreiro, J., González Cuadra, P., Abati, J., Castiñeiras, P., Fernández-Suárez, J., Sánchez Martínez, S., Andonaegui, P., González Clavijo, E., Díez Montes, A., Rubio Pascual, F.J., Valle Aguado, B., 2007. Space and time in the tectonic evolution of the northwestern Iberian Massif. Implications for the Variscan belt. In: Hatcher, R.D., Carlson, M.P., Mcbride, J.H., Martínez Catalán, J.R. (Eds.), 4-D Framework of Continental Crust. Geological Society of America Memoir, Boulder, Colorado, pp. 403–423.

Martínez Catalán, J.R., Arenas, R., Abati, J., Sánchez Martínez, S., Díaz García, F., Fernández-Suárez, J., González Cuadra, P., Castineiras, P., Gómez Barreiro, J., Díez Montes, A., González Clavijo, E., Rubio Pascual, F.J., Andonaegui, P., Jeffries, T.E., Alcock, J.E., Díez Fernández, R., López Carmona, A., 2009. A rootless suture and the loss of the roots of a mountain chain: the Variscan belt of NW Iberia. Comptes Rendus Geoscience 341 (2–3), 114–126.

Meireles, C.A.P., 2000. Carta Geológica de Portugal, 1:50000, Folla 3-D, Espinhosela. Instituto Geológico e Mineiro, Lisboa, 64.

Ménot, R.P., Peucat, J.J., Scarenzi, D., Piboule, M., 1988. 496 My age of plagiogranites in the Chamrousse ophiolite complex (external crystalline massifs in the French Alps): evidence of a lower Paleozoic oceanization. Earth and Planetary Science Letters 88, 82–92.

Montero, P., Floor, P., Corretge, L.G., 1998. The accumulation of rare-earth and high-field-strength elements in peralkaline granitic rocks: the Galineiro orthogneissic complex, northwestern Spain. The Canadian Mineralogist 36, 683–700.

Montero, P., Bea, F., Corretge, L.G., Floor, P., Whitehouse, M.J., 2009a. U–Pb ion microprobe dating and Sr and Nd isotope geology of the Galiñeiro Igneous Complex A model for the peraluminous/peralkaline duality of the Cambro-Ordovician magmatism of Iberia. Lithos 107 (3–4), 227–238.

Montero, P., Talavera, C., Bea, F., Lodeiro, F.G., Whitehouse, M.J., 2009b. Zircon geochronology of the Ollo de Sapo Formation and the age of the Cambro-Ordovician rifting in Iberia. Journal of Geology 117 (2), 174–191.

Morag, N., Avigad, D., Gerdes, A., Belousova, E., Harlavan, Y., 2011. Crustal evolution and recycling in the northern Arabian–Nubian Shield: new perspectives from zircon Lu–Hf and U–Pb systematics. Precambrian Research 186 (1–4), 101–116.

Murphy, J.B., Gutiérrez-Alonso, G., Fernández-Suárez, J., Braid, J.A., 2008. Probing crustal and mantle lithosphere origin through Ordovician volcanic rocks along the Iberian passive margin of Gondwana. Tectonophysics 461 (1–4), 166–180.

Murphy, J.B., Nance, R.D., Gutierrez-Alonso, G., Keppie, J.D., 2009. Supercontinent reconstruction from recognition of leading continental edges. Geology 37 (7), 595–598.

Nance, R.D., Murphy, J.B., Keppie, J.D., 2002. A Cordilleran model for the evolution of Avalonia. Tectonophysics 352 (1–2), 11–31.

Nance, R.D., Gutiérrez-Alonso, G., Keppie, J.D., Linnemann, U., Murphy, J.B., Quesada, C., Strachan, R.A., Woodcock, N.H., 2010. Evolution of the Rheic Ocean. Gondwana Research 17 (2–3), 194–222.

Narebski, W., Dostal, J., Dupuy, C., 1986. Geochemical characteristics of Lower Paleozoic spilite–keratophyre series in the Western Sudetes (Poland): petrogenetic and tectonic implications. Neues Jahrbuch für Mineralogie, Abhandlungen 155.

Nohda, S., Tatsumi, Y., Otofuji, Y., 1988. Asthenospheric injection and back-arc opening. Chemical Geology 68, 317–327.

Pedro, J., Araújo, A., Fonseca, P., Tassinari, C., Ribeiro, A., 2010. Geochemistry and U–Pb zircon age of the internal Ossa-Morena zone ophiolite sequences: a remnant of Rheic Ocean in SW Iberia. Ofioliti 35 (2), 117–130.

Pin, C., Carme, F., 1987. A Sm–Nd isotopic study of 500 Ma old oceanic crust in the Variscan belt of Western Europe: the Chamrousse ophiolite complex, Western Alps (France). Contributions to Mineralogy and Petrology 96 (3), 406–413.

Pin, C., Marini, F., 1993. Early Ordovician continental break-up in Variscan Europe: Nd–Sr isotope and trace element evidence from bimodal igneous associations of the Southern Massif central, France. Lithos 29, 177–196.

Pin, C., Cuesta, L.A.O., Gil Ibarguchi, J.I., 1992. Mantle-derived, Early Paleozoic A-type metagranitoids from the NW Iberian Massif—Nd isotope and trace-element constraints. Bulletin de la Societe Geologique de France 163 (4), 483–494.

Pollock, J.C., Wilton, D.H.C., van Staal, C.R., Morrissey, K.D., 2007. U–Pb detrital zircon geochronological constraints on the Early Silurian collision of Ganderia and Laurentia along the Dog Bay Line: the terminal Iapetan suture in the Newfoundland Appalachians. American Journal of Science 307 (2), 399–433.

Prigmore, J.K., Butler, A.J., Woodcock, N.J., 1997. Rifting during separation of Eastern Avalonia from Gondwana. Evidence from subsidence analyses. Geology 25, 203–206.

Raddick, M.J., Parmentier, E.M., Scheirer, D.S., 2002. Buoyant decompression melting: a possible mechanism for intraplate volcanism. Journal of Geophysical Research 107 (B10), 2228.

Ribeiro, M.L., Floor, P., 1987. Magmatismo peralcalino no Macico Hesperico: Sua distribuico e significado geodinamico, geologia de los granitoides y rocas asociadas del Macizo Hesperico. In: C. Bea, F.E., Gonzalo, J.C., López Plaza, M., Rodríguez, M.D. (Eds.), Geología de los granitoides y rocas asociadas del Macizo Hespérico : libro homenaje a L. C. García de Figuerola. Ediciones Rueda, Madrid, pp. 211–222.

Ribeiro, A., Pereira, E., Dias, R., 1990. Structure in the northwest of the Iberian Peninsula. In: Dallmeyer, R.D., Martínez García, E. (Eds.), Pre-Mesozoic geology of Iberia. Springer-Verlag, Berlin, pp. 220–236.

Ricci, C.A., Sabatini, G., 1978. Petrogenetic affinity and geodynamic significance of metabasic rocks from Sardinia, Corsica and Provence. Neues Jahrbuch für Mineralogie, Monatshefte 1, 28–38.

Ringwood, A.E., Irifune, T., 1988. Nature of the 650-km seismic discontinuity: implications for mantle dynamics and differentiation. Nature 331, 131–136.

Rodríguez Aller, J., 2005. Recristalización y deformación de litologías supracorticales sometidas a metamorfismo de alta presión (Complejo de Malpica-Tuy, NO del Macizo Ibérico). : Nova Terra, 29. Instituto de Xeoloxía Isidro Parga Pondal, A Coruña, Spain (410 pp.).

Rodríguez, J., Paquette, J.L., Gil Ibarguchi, J.I., 2007. U–Pb dating of Lower Ordovician alkaline magmatism in the Gondwana margin (Malpica–Tui complex, Iberian Massif): latest continental events before oceanic spreading. In: Arenas, R., Martínez Catalán, J.R., Abati, J., Sánchez Martínez, S. (Eds.), IGCP 497—The Rheic Ocean: its origin, evolution and correlatives. The rootless Variscan suture of NW Iberia (Galicia, Spain). Field trip guide & Conference abstracts. Instituto Geologico y Minero de Espana, A Coruña, Spain, pp. 163–164.

Rodríguez-Alonso, M.D., Peinado, M., Lopez-Plaza, M., Franco, P., Carnicero, A., Gonzalo, J.C., 2004. Neoproterozoic–Cambrian synsedimentary magmatism in the Central Iberian Zone (Spain): geology, petrology and geodynamic significance. International Journal of Earth Sciences 93 (5), 897–920.

Rohrman, M., van der Beek, P.A., Van Der Hilst, R.D., Reemst, P., 2002. Timing and mechanisms of North Atlantic Cenozoic uplift: evidence for mantle upwelling. Geological Society, London, Special Publications 196 (1), 27–43.

Sánchez Martínez, S., Arenas, R., Fernández-Suárez, J., Jeffries, T.E., 2009. From Rodinia to Pangaea: ophiolites from NW Iberia as witness for a long-lived continental margin. Geological Society, London, Special Publication 327, 317–341.

Sánchez Martínez, S., Arenas, R., Gerdes, A., Castiñeiras, P., Potrel, A., Fernández-Suárez, J., 2011. Isotope geochemistry and revised geochronology of the Purrido Ophiolite (Cabo Ortegal Complex, NW Iberian Massif): Devonian magmatism with mixed sources and involved Mesoproterozoic basement. Journal of the Geological Society 168 (3), 733–750.

Santos Zalduegui, J.F., Scharer, U., Gil Ibarguchi, J.I., 1995. Isotope constraints on the age and origin of magmatism and metamorphism in the Malpica-Tuy allochthon, Galicia, NW Spain. Chemical Geology 121 (1–4), 91–103.

Sleep, S.H., Toksöz, M.N., 1971. Evolution of marginal basins. Nature 33, 548–550.

Solá, A.R., Montero, P., Ribeiro, M.L., Neiva, A.M.R., Zinger, T., Bea, F., 2005. Pb/Pb zircon age of Carrascal Massif, central Portugal. Geochimica et Cosmochimica Acta 69 (10), Supplement 1, Goldschmidt Conference Abstracts 2005., A856.

Solá, A.R., Pereira, M.F., Williams, I.S., Ribeiro, M.L., Neiva, A.M.R., Montero, P., Bea, F., Zinger, T., 2008. New insights from U–Pb zircon dating of Early Ordovician magmatism on the northern Gondwana margin: the Urra Formation (SW Iberian Massif, Portugal). Tectonophysics 461 (1–4), 114–129.

Sommer, H., Gauert, C., 2011. Hydrating laterally extensive regions of continental lithosphere by flat subduction: a pilot study from the North American Cordillera. Journal of Geodynamics 51 (1), 17–24.

Stacey, J.S., Kramers, J.D., 1975. Approximation of terrestrial lead isotope evolution by a 2-stage model. Earth and Planetary Science Letters 26 (2), 207–221.

Stampfli, G.A., Von Raumer, J.F., Borel, G., 2002. Paleozoic evolution of pre-Variscan terranes: from Gondwana to the Variscan collision. In: Martínez Catalán, J.R., Hatcher, J.R.D., Arenas, R., Díaz García, F. (Eds.), Variscan–Appalachian Dynamics: The Building of the Late Paleozoic Basement. Geological Society of America Special Paper, Boulder, Colorado, pp. 263–280.

Stampfli, G.M., von Raumer, J., Wilhem, C., 2011. The distribution of Gondwana derived terranes in the early Paleozoic. In: Gutiérrez-Marco, J.C., Rábano, I., García-Bellido,

D. (Eds.), The Ordovician of the World. Cuadernos del Museo Geominero, Madrid, pp. 567–574.
Talavera, C., Bea, F., Montero, P., Whitehouse, M.J., 2008. A revised Ordovician age for the Sisargas orthogneiss, Galicia (Spain). Zircon U–Pb ion-microprobe and LA-ICPMS dating. Geologica Acta 6 (4), 313–317.
Tatsumi, Y., Maruyama, S., Nohda, S., 1990. Mechanism of backarc opening in the Japan Sea: role of asthenospheric injection. Tectonophysics 181, 299–306.
Timmermann, H., Dörr, W., Krenn, E., Finger, F., Zulauf, G., 2006. Conventional and in situ geochronology of the Tepla Crystalline unit, Bohemian massif: implications for the processes involving monazite formation. International Journal of Earth Sciences, 95, pp. 629–648.
Toksöz, M.N., Hsui, A.T., 1978. Numerical studies of back-arc convection and the formation of marginal basins. Tectonophysics 50 (2–3), 177–196.
Ulmer, P., 2001. Partial melting in the mantle wedge—the role of H_2O in the genesis of mantle-derived "arc-related" magmas. Physics of the Earth and Planetary Interiors 127, 215–232.
Valverde-Vaquero, P., Dunning, G.R., 2000. New U–Pb ages for Early Ordovician magmatism in Central Spain. Journal of the Geological Society 157, 15–26.
Valverde-Vaquero, P., Marcos, A., Farias, P., Gallastegui, G., 2005. U–Pb dating of Ordovician felsic volcanism in the Schistose Domain of the Galicia-Trás-os-Montes Zone near Cabo Ortegal (NW Spain). Geologica Acta 3, 27–37.
Van Calsteren, P.W.C., Boelrijk, N., Hebeda, E.H., Priem, H.N.A., Dentex, E., Verdurmen, E.A.T., Verschure, R.H., 1979. Isotopic dating of older elements (including the Cabo Ortegal mafic–ultramafic complex) in the Hercynian orogen of NW Spain—manifestations of a presumed Early Paleozoic mantle–plume. Chemical Geology 24 (1–2), 35–56.
van der Lee, S., Regenauer-Lieb, K., Yuen, D.A., 2008. The role of water in connecting past and future episodes of subduction. Earth and Planetary Science Letters 273 (1–2), 15–27.
von Raumer, J.F., Stampfli, G.M., 2008. The birth of the Rheic Ocean–Early Palaeozoic subsidence patterns and subsequent tectonic plate scenarios. Tectonophysics 461 (1–4), 9–20.
Von Raumer, J.F., Stampfli, G.M., Borel, G., Bussy, F., 2002. Organization of pre-Variscan basement areas at the north-Gondwanan margin. International Journal of Earth Sciences 91 (1), 35–52.
von Raumer, J.F., Stampfli, G.M., Hochard, C., Gutiérrez-Marco, J.C., 2006. The Early Palaeozoic in Iberia a plate-tectonic interpretation. Zeitschrift der Deutschen Gesellschaft für Geowissenschaften 157 (4), 575–584.
Williams, I.S., 1997. U–Th–Pb geochronology by ion microprobe: not just ages but histories. Economic Geology 7, 1–35.
Yamamoto, T., Hoang, N., 2009. Synchronous Japan Sea opening Miocene fore-arc volcanism in the Abukuma Mountains, NE Japan: an advancing hot asthenosphere flow versus Pacific slab melting. Lithos 112 (3–4), 575–590.
Zhao, D., Maruyama, S., Omori, S., 2007. Mantle dynamics of Western Pacific and East Asia: insight from seismic tomography and mineral physics. Gondwana Research 11 (1–2), 120–131.